Photonic structures in biology

Pete Vukusic and J. Roy Sambles

Thin Film Photonics, School of Physics, Exeter University, Exeter EX4 4QL, UK (e-mail: P.Vukusic@ex.ac.uk)

Millions of years before we began to manipulate the flow of light using synthetic structures, biological systems were using nanometre-scale architectures to produce striking optical effects. An astonishing variety of natural photonic structures exists: a species of Brittlestar uses photonic elements composed of calcite to collect light, *Morpho* butterflies use multiple layers of cuticle and air to produce their striking blue colour and some insects use arrays of elements, known as nipple arrays, to reduce reflectivity in their compound eyes. Natural photonic structures are providing inspiration for technological applications.

The natural world has exploited photonic structures since the Cambrian explosion: the sudden and enormous diversification of life that accompanied the start of the Cambrian period over 500 million years ago. Evidence from this era suggests that the co-development of predator and prey colouration, in step with their visual systems, resulted in the evolution of various life forms. Light can be a significant selection pressure for the evolution of certain animal groups, leading to the astonishing diversity of natural photonic structures present in the world today. Such structures might provide the inspiration for future technological applications.

Photonic structures in aquatic systems

Decades before the synthesis of fabricated photonic structures, studies were revealing the complex and elegant way in which it was accomplished naturally. Aquatic systems were the subject of many of the earliest studies. Crystal multilayer structures of guanine were identified as the key component of coloured and broad-band silver reflections in many fish and also found to be a high-reflectance element in many bioluminescent organs and a sub-retinal component that assists with specialized marine vision[1]. Recent interest in aquatic systems has revealed photonic structures of astonishing complexity. For example, arm ossicles from light-sensitive species of brittlestar, *Ophiocoma wendtii*, have regular arrays of inorganic microstructures (Fig. 1a) with a characteristic double-lens design[2] (Fig. 1b). These microlenses are photonic elements, each composed of single anisotropic calcite crystals that focus light towards nerve bundles of photoreceptors 4–7 μm below them inside the arm ossicle tissue. The design of the surface of each lens and the orientation of constituent calcite minimizes spherical aberration and birefringence that might otherwise degrade the optical function. Such microlens arrays assist in creating levels of light and shadow sensitivity that may serve to warn of the presence of predators.

Equally fascinating are the nanostructures found in the hair-like setae of many species of polychaete worm (Fig. 2a). In these creatures, a two-dimensional (2D) hexagonal lattice of voids within the cross-section of each seta (Fig. 2b) creates a natural pseudo-photonic crystal fibre along its full length[3,4]. The high spatial periodicity of this lattice (Fig. 2c, d) generates a partial photonic bandgap (PBG) by which colour is strongly Bragg-scattered in certain directions. As a consequence of this, strong iridescence is observed laterally. The biological significance of the colour, and therefore of the intricate structure, is understood to be visibility; this contrasts with the principal design purpose of recently developed synthetic photonic crystal fibres, which is to guide light longitudinally[5]. The absence of centrally located defects within the natural photonic fibres examined so far, prevents light-guiding in these setae.

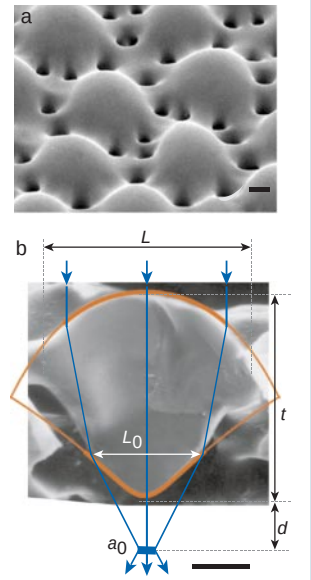

Figure 1 Peripheral layer of ophiocomid brittlestars. **a**, Scanning electron micrographs (SEM) of the peripheral layer of a dorsal arm plate from the brittlestar *Ophiocoma wendtii* showing the microlens array. **b**, SEM of an individual lens in *O. wendtii*. The functional region of this lens (L_0) closely matches the profile of a lens that is compensated for spherical aberration (represented by the red lines). The light paths are shown in blue (images reproduced with permission from J. Aizenberg). Bars, 10 μm.

Photonic structures in insects and birds

Iridescence is much more commonly encountered in terrestrial systems than in aquatic systems. The photonics associated with brightly coloured birds and insects has been extensively studied for over a century but only recently have significant advances been made. Discoveries of partial PBG structures in Coleoptera and Lepidoptera highlight the breadth of nature's innovative use of light. Although certain systems, among them species of Coleoptera[6] and Hymenoptera[7], display subtle colouration as a result of diffraction from surface periodicities, the majority of strong photonic effects arise in species that have evolved structures that have layers of alternately high and low refractive index. This leads to optical interference: an effect that pervades much of modern optics and the physics of which is well understood[8].

In iridescent blue *Morpho rhetenor* butterflies (Fig. 3a), ultralong-range visibility of up to half a mile is attributed to photonic structures formed by discrete multilayers of

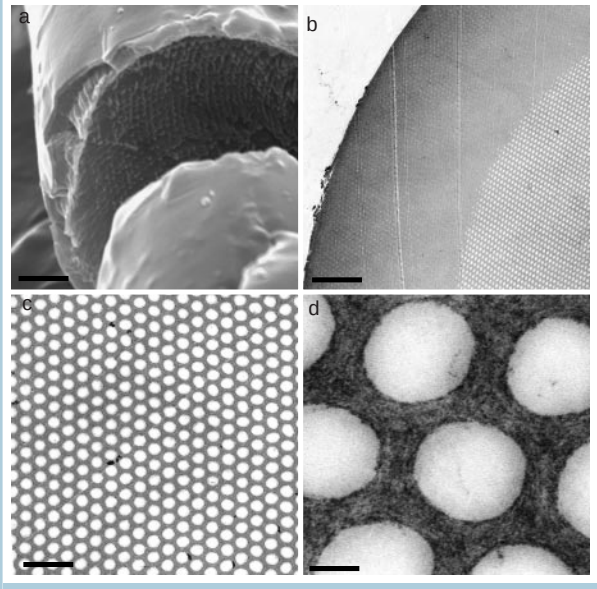

Figure 2 Iridescent setae from polychaete worms. **a**, Scanning electron micrograph (SEM) and **b**–**d**, transmission electron micrograph (TEM) images of transverse sections through a single iridescent seta. Bars, **a**, 2 μm; **b**, 5 μm; **c**, 1 μm; **d**, 120 nm.

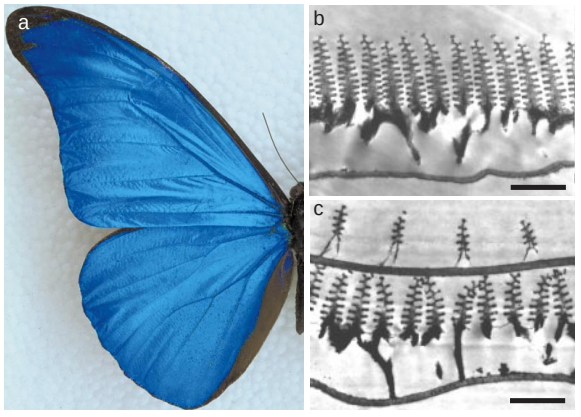

Figure 3 Iridescence in the butterfly *Morpho rhetenor*. **a**, Real colour image of the blue iridescence from a *M. rhetenor* wing. **b**, Transmission electron micrograph (TEM) images showing wing-scale cross-sections of *M. rhetenor*. **c**, TEM images of a wing-scale cross-section of the related species *M. didius* reveal its discretely configured multilayers. The high occupancy and high layer number of *M. rhetenor* in **b** creates an intense reflectivity that contrasts with the more diffusely coloured appearance of *M. didius*, in which an overlying second layer of scales effects strong diffraction[4]. Bars, **a**, 1 cm; **b**, 1.8 μm; **c**, 1.3 μm.

cuticle and air[9,10] (Fig. 3b, c). Photonic structures of reduced dimensions, present in certain *Colias* butterflies, effect intense UV visibility[11]. In other species of butterfly, orientational adjustments to the alignment of such discrete multilayers produce strong angle-dependent iridescence that provides high-contrast colour flicker with minimal wing movement[12] or strong iridescence at grazing incidence when viewed posteriorly[13].

The discrete layering in the examples above contrasts with the more continuous layering, which appears to have developed primarily to induce cryptic colouration, in other butterfly species. In certain architectures, this may not only bring about colour stimulus synthesis[14] but also strong linearly polarized reflection of a specific colour, an effect that contributes to intraspecific communication[15]. Several species accomplish this using a multilayered structure embedded in 2D arrays of deep concavities (Fig. 4a, b); this design enables the reflection of yellow light at normal incidence from the base of each concavity and blue light through a double reflection from opposite and perpendicularly inclined sides of each concavity (Fig. 4c) to produce a blue annulus with a yellow centre[16] (Fig. 4d). The juxtaposition of these two colours synthesizes the green colouration perceived by the human eye—and possibly by the predator's.

Certain Coleoptera, however, exhibit continuously layered exocuticle that strongly reflects circularly polarized light through an analogue of optically active cholesteric liquid crystalline structures. The helical arrangement of chitin microfibrils that make up such exocuticle, and which are systematically rotated by a small amount across successive planes, creates a periodicity that produces circularly polarized coloured reflection[17]. In other words, the polarized reflection is not derived from optical rotation at a molecular level from the L-amino acids of the cuticle protein and the D-amino sugars of the chitin; instead it arises at the supermolecular level and is similar to that exhibited by a cholesteric liquid crystal from the rotation of the local average alignment direction of the liquid crystal molecules (the director). Although similar helical structures are found in many other iridescent species, they are rarely responsible for similarly strong colouration and anomalous polarization properties[4].

Structurally coloured avian feather barbs and integument, although they exhibit less structural diversity than scales of Lepidoptera, are no less remarkable. Recent analyses suggest that such colour as is seen in many Avian orders, is the product of coherent, rather than incoherent, scatter from the spatial variation in refractive index of medullary keratin in feather barbs or of collagen fibres in the dermis[18].

Photonics in flora

Advanced photonic development is not limited to fauna. Certain anomalous species of flora also show partial PBGs that underpin an often vivid structural colour[19] (Fig. 5a). Invariably this is mediated by variations in 1D multilayering (although more complex structural designs are also thought to exist), producing iridescence in vascular plant leaves, fruits and marine algae[4]. Periodicity is generally formed by laminations of hydrated cellulose, which are usually located close

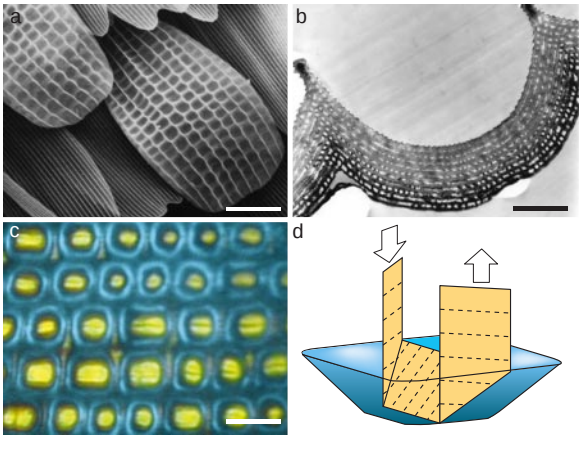

Figure 4 Iridiscence in *Papilo palinurus*. **a**, SEM of an iridescent scale showing its array of concavities, each with a section that exhibits the curved multilayering shown by transmission electron micrography in **b**. This structure produces two simultaneous structural colours **c**, yellow and blue . **d**, The blue annulus is created by a double reflection from opposite and perpendicular concavity sides. **d** also schematically illustrates the way in which incident linearly polarized blue light has its e-vector (dotted lines) rotated by this double reflection. Bars, **a**, 15 μm; **b**, 1 μm; **c**, 6 μm.

to epidermal cell walls or within elongated chloroplasts, but it can also be the result of a helical arrangement of cellulose fibrils (Fig. 5b). Iridescence in leaves is thought to produce particular intensity ratios of incident radiation bands that can penetrate to phytochrome centres and thus affect the development of the plant, although the photonic effect may have other functions. Structural colour in fruit skin reduces post-maturation discolouration and ultimately improves dispersal[20]. Interestingly too, convexly curved epidermal cells on the surface of several particular species of plant appear to act as microlenses[21], resulting in increased photosynthetic flux density on specially oriented chloroplasts at specific depths within the plants' leaves.

Photonic crystal structures

Natural systems also exist that employ remarkable 3D photonic crystals of cuticle (Fig. 6a, b) to produce partial PBGs, with the effect that bright colour is reflected over a broad angle[4]. From the perspective of modern photonic technology, this indicates an evolutionary step further along the photonic road, since, in principle, 3D periodicity potentially manipulates the flow of light in all directions. The physical structure of such photonic crystals, although varying somewhat between species of examined Lepidoptera, appears consistently to be approximately tetrahedral[22,23]. Interestingly, bandgap calculations indicate that a perfect tetrahedral configuration offers the highest reflectivity over the broadest angle for a given refractive index contrast between component media[24]. The physical design of this photonic structure has converged towards one of the most optically efficient configurations. Additionally, the selective advantage of using this microstructure rather than a surface grating or a multilayer system, excluding physiological considerations, is that it can be incorporated into multiple neighbouring domains (Fig. 6c), each orientated slightly differently, to produce a macroscopic colour that is completely independent of the viewing angle[4].

In contrast to such scattering from a honeycombed lattice of voids described above, other Lepidopteran systems employ randomly orientated solid ellipsoids to produce a multiwavelength scatter that creates the appearance of being white. More eyecatching, however, are the colour centres that arise via Bragg diffraction from 3D lattices of closely packed with solid spheres with high refractive indices. These

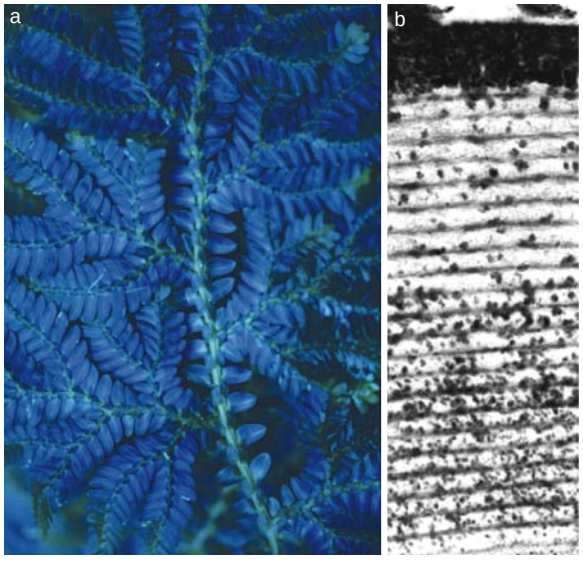

Figure 5 Structural colour in flora. **a**, Blue iridescence is prevalent in the fern-like tropical understory plants of the genus *Selaginella*. **b**, TEM section of a juvenile leaf from the plant *Diplazium tomentosum*. (Both images reproduced with permission from D. Lee.)

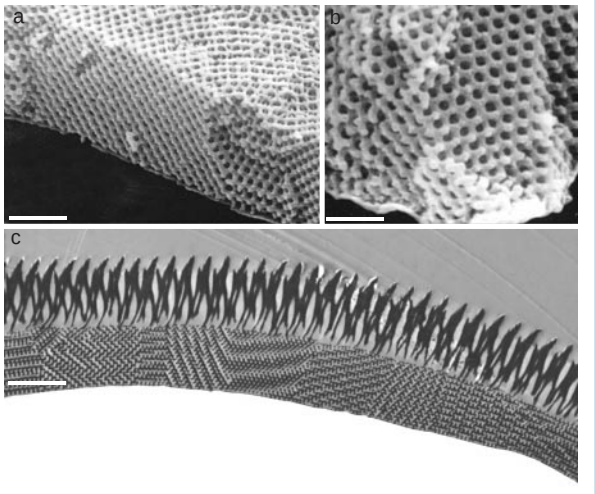

Figure 6 The green colour of *Parides sesostris* is created by a photonic crystal. **a**, **b**, SEMs of the exposed photonic crystal after the superficial ridging has been removed. **c**, a TEM showing a 50 nm section through the scale shown in a; the ridging is intact whereas the neighbouring but differently oriented domains of identical 3D structure are distinguished by contrasting 2D patterns (here, the darkly contrasted material is cuticle). Bars, **a**, 1.2 μm; **b**, 750 μm; **c**, 2.5 μm.

lattices have recently been discovered in the iridescent cuticle of certain beetle species (A. R. Parker, V. L. Welch & D. Driver, personal communication), but the effect is far better understood in the inanimate structures associated with gem opals. In these, strong coloured regions are created by aggregates of 150–350 nm diameter amorphous silica spheres arranged hexagonally in layers that are usually stacked randomly. Some opal specimens exhibit parallel domains of ordered packing that are commonly face-centered cubic but which occasionally are hexagonally close-packed[25]. This ordered structure is understood to be the result of precipitative settling of silica gel solution: the opal's colouring is purely artefactual.

Anti-reflection structures

Although the character of most natural partial PBG systems is associated with bright colour or broad angle reflectivity, a specific form of nanostructure minimizes reflectivity at a surface over broad angles or frequency ranges. The structure gradually matches the optical impedance of one medium with that of its neighbour across the interface. This is invariably achieved by incorporation of arrays of tapered elements, described as nipple arrays, across the boundary. Considerable research into such nipple arrays, which are commonly found on arthropodal ommatidial surfaces (Fig. 7a), suggests a distinct visual selection advantage associated with their use in compound eyes[26]: the reduced reflectivity from the ommatidial surface enhances the photon collection efficiency of the visual system. The evolutionary development of these anti-reflective nanostructures must have occurred very early—they have been found on the ommatidial surfaces of amber-trapped diptera from the Eocene period[27]. Further evidence that these photonic structures enhance transmission through interfaces comes from their presence on the dorsal and ventral surfaces of transparent diurnal moth wings[28] (Fig. 7b). Additionally, they are seen to remove the Brewster-mediated disparity in reflection of different polarizations from the wing (P.V. and J.R.S., unpublished data), a relevant feature within a forum where visual polarization sensitivity is ubiquitous[15,29].

As well as enhancing transparency in certain insects, nanostructures may be associated with the colour black on certain lepidopteran wing scales. Although the dark melanin-based pigmentation in such scales is the absorbing medium, optical scattering

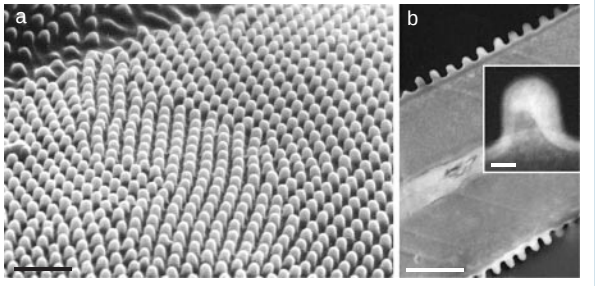

Figure 7 Anti-reflective nipple arrays. **a**, The anti-reflective nipple arrays on ommatidial surfaces of a lepidopteran eye appear identical to those found (**b**) on the transparent wings of certain hawkmoths. This image shows a transparent wing section with a nipple array on both surfaces. The inset image shows the magnified profile of a single nipple. Bars, **a**, 1 μm; **b**, 1 μm; inset, 100 nm.

from specific tapered nanostructures on and within each scale significantly increases incident light absorption by the pigment and subsequently enhances the visual appearance of the blackness (P.V., J.R.S. and C. R. Lawrence, unpublished data).

Future considerations

Numerous studies, many of them very recent, have sought to discover and characterize the photonics associated with natural specimens. Many of the revealed designs have existed naturally for millennia, but were, until recently, considered to be the product of contemporary technological innovation. Despite considerable advances in our understanding, significant weaknesses persist. Not enough is known about the material used in these natural systems, particularly with reference to their real and imaginary refractive index component dispersion properties across relevant frequency ranges. Additionally, the sheer physical complexity of many natural systems often renders an accurate representation of their structure extremely difficult. Rigorous application of electromagnetic grating theory[30], which increasingly uses modelling in finite element form, is beginning to address some of this complexity.

Natural systems offer technologically unrealized photonic structures and design protocols. Although they have evolved for specific biological purposes and comprise physiologically constrained constituent materials, they provide inspiration for technological applications that require UV, visible, IR or microwave frequency bands. Adaptive replication of certain natural structures, using commercially available materials with better suited optical properties, is already yielding marketable benefit. The range of these replicated structures, and potential future applications, varies, from those associated with advanced optical properties of paints, fabrics and displays to anti-reflection of UV and visible light in electro-optical components and of microwaves from large surfaces, to the intrinsic photonic lasing and light-guiding components associated with optical processing. Present manufacturing techniques such as thin layer vacuum deposition, template embossing and various forms of lithography are limited and often prohibitively expensive. It is for this reason that the biological processes of manufacture are of great interest. Invariably, these structures are self-assembled in a range of environments—in pupae, eggs or during early growth—through design templates that are often influenced by environmental factors[31] but are ultimately controlled at the genetic level. Although many natural photonic structures may not be technologically appropriate for direct use, genetic manipulation may one day yield directly exploitable photonic components. □

doi:10.1038/nature01941

1. Denton, E. J. Reflectors in fishes. *Sci. Am.* **224,** 64–72 (1971).
2. Aizenberg, J., Tkachenko, A., Weiner, S., Addadi, L. & Hendler, G. Calcitic microlenses as part of the photoreceptor system in brittlestars. *Nature* **412,** 819–822 (2001).
3. Parker, A. R., McPhedran, R. C., McKenzie, D. R., Botten, L. C. & Nicorovici, N. A. Photonic engineering: Aphrodite's iridescence. *Nature* **409,** 36–37 (2001).
4. Vukusic, P. in *Optical Interference Coatings* (eds Kaiser, N. & Pulker, H. K.) 1-34 (Springer, New York, 2003).
5. Knight, J. C. & Russell, P. St. J. Photonic Crystal Fibers: New Ways to Guide Light. *Science* **296,** 276–277 (2002).
6. Parker, A. R. Diffracting optics in animals: diversity and biological significance. *Eur. Opt. Soc. Top. Meet. Digest Series* **18**, 27–30 (1998).
7. Hinton, H. E., Gibbs, D. F. & Silberglied, R. Stridulatory files as diffraction gratings in mutillid wasps. *J. Insect Physiol.* **15,** 549–552 (1969).
8. Kaiser, N. & Pulker, H. K. (eds) *Optical Interference Coatings*. (Springer, New York, 2003).
9. Vukusic, P., Sambles, J. R., Lawrence, C. R. & Wootton, R. J. Quantified interference and diffraction in single *Morpho* butterfly scales. *Proc. R. Soc. Lond. B* **266,** 1402–1411 (1999).
10. Kinoshita, S., Yoshioka, S. & Kawagoe, K. Mechanisms of structural colour in the *Morpho* butterfly: cooperation of regularity and irregularity in an iridescent scale. *Proc. R. Soc. Lond. B.* **269,** 1417–1421 (2002).
11. Ghiradella, H. Light and colour on the wing: Structural colours in butterflies and moths. *Appl. Opt.* **30,** 3492–3500 (1991).
12. Vukusic, P., Sambles, J. R., Lawrence, C. R. & Wootton, R. J. Structural colour: Now you see it – now you don't. *Nature* **410,** 36 (2001).
13. Lawrence, C. R., Vukusic, P. & Sambles, J. R. Grazing incidence iridescence from a butterfly wing. *Appl. Opt.* **41,** 437–441 (2002).
14. Agoston, G. A. *Colour Theory and its Applications in Art and Design* (Springer, New York 1987).
15. Sweeney, A., Jiggins, C. & Johnsen, S. Polarized light as a butterfly mating signal. *Nature* **423**, 31–32 (2003).
16. Vukusic, P., Sambles, J. R. & Lawrence, C. R. Colour mixing in wing scales of a butterfly. *Nature* **404,** 457 (2000).
17. Neville, A. C. & Caveney, S. Scarabeid beetle exocuticle as an optical analogue of cholesteric liquid crystals. *Biol. Rev.* **44,** 531–562 (1969).
18. Prum, R. O. & Torres, R. H. Structural colouration of avian skin: convergent evolution of coherently scattering dermal collagen arrays. *J. Exp. Biol.* **206,** 2409–2429 (2003).
19. Lee, D. W. Iridescent blue plants. *Am. Sci.* **85,** 56–63 (1997).
20. Lee, D. W. Ultrastructural basis and function of iridescent blue color of fruits in *Elaeocarpus*. *Nature* **349,** 260–262 (1991).
21. Bone, R. A., Lee, D. W. & Norman, J. M. Epidermal cells functioning as lenses in leaves of tropical rain-forest shade plants. *Appl. Opt.* **24,** 1408–1412 (1985).
22. Vukusic, P. Shedding light on butterfly wings. *Proc. SPIE* **4438**, 85–95 (2001).
23. Argyros, A., Manos, S., Large, M. C. J., McKenzie, D. R., Cox G. C. & Dwarte, D. M. Electron tomography and computer visualisation of a three-dimensional 'photonic' crystal in a butterfly wing-scale. *Micron* **33,** 483–487 (2002).
24. Chan, C. T., Ho, K. M. & Soukoulis, C. M. Photonic band gaps in experimentally realizable periodic dielectric structures. *Europhys. Lett.* **16,** 563–568 (1991).
25. Sanders, J. V. & Darragh, P. J. The microstructure of precious opal. *The Mineralogical Record* **2**, 261–268 (1971).
26. Land M. F. & Nilsson, D. E. *Animal Eyes*. (Oxford Univ., Oxford, 2001).
27. Parker, A. R., Hegedus, Z. & Watts, R. A. Solar-absorber antireflector on the eye of an Eocence fly (45 Ma). *Proc. Roy. Soc. B,* **265**, 811–815 (1998).
28. Yoshida, A., Motoyama, M., Kosaku, A. & Miyamoto K. Antireflective nanoproturberance array in the transparent wing of a hawkmoth *Cephanodes hylas*. *Zool. Sci.* **14,** 737–741 (1997).
29. Wehner, R. Polarization vision – a uniform sensory capacity? *J. Exp. Biol.* **204,** 2589–2596 (2001).
30. Gralak, B., Tayeb, G. & Enoch, S. *Morpho* butterflies wings color modeled with lamellar grating theory. *Opt. Express* **9,** 567–578 (2001).
31. McMillan, W. O., Monteiro, A. & Kapan, D. D. Development and evolution on the wing. *Trends Ecol. Evol.* **117,** 125–133 (2002).

2.3 Å resolution. The crystal belongs to space group $P2_1$, with cell dimensions of $a = 57.3$ Å, $b = 66.4$ Å, $c = 90.0$ Å and $\beta = 103.1°$. For the β_4 core crystal, a 3.0 Å resolution data set was collected. The crystal also belongs to space group $P2_1$, but is non-isomorphous with that of β_3 core, with cell dimensions of $a = 60.3$ Å, $b = 83.2$ Å, $c = 72.3$ Å and $\beta = 94.9°$. The data set for the β_3 core–AID crystal was collected to 2.6 Å resolution. It belongs to space group $C2$, with cell dimensions of $a = 252.3$ Å, $b = 69.0$ Å, $c = 60.7$ Å and $\beta = 96.7°$. There are two molecules in the asymmetric unit for all three crystals, giving a V_m (Matthew's coefficient) of 2.0 Å^3 Da^{-1}, 2.3 Å^3 Da^{-1} and 2.9 Å^3 Da^{-1}, respectively. All diffraction data were collected at the X4A beamline of the Brookhaven National Laboratory. The diffraction images were processed and scaled with the HKL package[22]. The data processing statistics are summarized in Supplementary Table 1.

Structure determination and refinement

The locations of Se atoms in the β_3 core crystal were determined with the program SOLVE[23]. Reflection phases to 2.3 Å resolution were calculated and improved with the same program, which also automatically located 50% of the residues in the molecule. The full atomic model was built into the electron density with the program O[24]. Structure refinement was carried out with the program CNS[25]. The structures of the β_3 core–AID complex and β_4 core were determined by the molecular replacement method with the program COMO[26] using the β_3 core structure as the model, and were refined as described above. The statistics on structural refinement are summarized in Supplementary Table 1. The current models fit the electron density map well and all main-chain dihedral angles are located in favourable regions on the Ramachandran plot (Supplementary Fig. 2).

Oocyte expression and electrophysiology

All constructs for oocyte expression were subcloned into variants of pGEMHE. cRNAs were synthesized *in intro* and injected in various combinations into *Xenopus* oocytes, which were obtained and maintained as described[27]. Two-electrode voltage-clamp recordings were performed as described[27]. Data are presented as mean ± s.d. (number of observations).

Received 5 March; accepted 10 May 2004; doi:10.1038/nature02641.
Published online 30 May 2004.

1. Catterall, W. A. Structure and regulation of voltage-gated Ca^{2+} channels. *Annu. Rev. Cell Dev. Biol.* **16,** 521–555 (2000).
2. Birnbaumer, L. *et al.* Structures and functions of calcium channel beta subunits. *J. Bioenerg. Biomembr.* **30,** 357–375 (1998).
3. Arikkath, J. & Campbell, K. P. Auxiliary subunits: essential components of the voltage-gated calcium channel complex. *Curr. Opin. Neurobiol.* **13,** 298–307 (2003).
4. Dolphin, A. C. β subunits of voltage-gated calcium channels. *J. Bioenerg. Biomembr.* **55,** 607–627 (2003).
5. De Waard, M., Pragnell, M. & Campbell, K. P. Ca^{2+} channel regulation by a conserved beta subunit domain. *Neuron* **13,** 495–503 (1994).
6. De Waard, M., Scott, V. E., Pragnell, M. & Campbell, K. P. Identification of critical amino acids involved in α1-β interaction in voltage-dependent Ca^{2+} channels. *FEBS Lett.* **380,** 272–276 (1996).
7. Pragnell, M. *et al.* Calcium channel β-subunit binds to a conserved motif in the I–II cytoplasmic linker of the α_1-subunit. *Nature* **368,** 67–70 (1994).
8. Canti, C. *et al.* Evidence for two concentration-dependent processes for β-subunit effects on α1B calcium channels. *Biophys. J.* **81,** 1439–1451 (2001).
9. Opatowsky, Y., Chomsky-Hecht, O., Kang, M. G., Campbell, K. P. & Hirsch, J. A. The voltage-dependent calcium channel beta subunit contains two stable interacting domains. *J. Biol. Chem.* **278,** 52323–52332 (2003).
10. Hanlon, M. R., Berrow, N. S., Dolphin, A. C. & Wallace, B. A. Modelling of a voltage-dependent Ca^{2+} channel beta subunit as a basis for understanding its functional properties. *FEBS Lett.* **445,** 366–370 (1999).
11. Hendrickson, W. A. Determination of macromolecular structures from anomalous diffraction of synchrotron radiation. *Science* **254,** 51–58 (1991).
12. Tavares, G. A., Panepucci, E. H. & Brunger, A. T. Structural characterization of the intramolecular interaction between the SH3 and guanylate kinase domains of PSD-95. *Mol. Cell* **8,** 1313–1325 (2001).
13. Zarrinpar, A., Bhattacharyya, R. P. & Lim, W. A. The structure and function of proline recognition domains. *Sci. STKE* **2003,** RE8 (2003).
14. Larson, S. M. & Davidson, A. R. The identification of conserved interactions within the SH3 domain by alignment of sequences and structures. *Protein Sci.* **9,** 2170–2180 (2000).
15. Blaszcyk, J., Li, Y., Yan, H. & Ji, X. Crystal structure of unligated guanylate kinase from yeast reveals GMP-induced conformational changes. *J. Mol. Biol.* **307,** 247–257 (2001).
16. Sheng, M. & Pak, D. T. Ligand-gated ion channel interactions with cytoskeletal and signaling proteins. *Annu. Rev. Physiol.* **62,** 755–778 (2000).
17. Beguin, P. *et al.* Regulation of Ca^{2+} channel expression at the cell surface by the small G-protein kir/Gem. *Nature* **411,** 701–706 (2001).
18. Finlin, B. S., Crump, S. M., Satin, J. & Andres, D. A. Regulation of voltage-gated calcium channel activity by the Rem and Rad GTPases. *Proc. Natl Acad. Sci. USA* **100,** 14469–14474 (2003).
19. McGee, A. W. *et al.* Structure of the SH3-guanylate kinase module from PSD-95 suggests a mechanism for regulated assembly of MAGUK scaffolding proteins. *Mol. Cell* **8,** 1291–1301 (2001).
20. Garcia, E. P. *et al.* SAP90 binds and clusters kainate receptors causing incomplete desensitization. *Neuron* **21,** 727–739 (1998).
21. Maximov, A., Sudhof, T. C. & Bezprozvanny, I. Association of neuronal calcium channels with modular adaptor proteins. *J. Biol. Chem.* **274,** 24453–24456 (1999).
22. Otwinowski, Z. & Minor, W. Processing of X-ray diffraction data collected in oscillation mode. *Methods Enzymol.* **276,** 307–326 (1997).
23. Terwilliger, T. C. & Berendzen, J. Automated MAD and MIR structure solution. *Acta Crystallogr. D* **55,** 849–861 (1999).
24. Jones, T. A., Zou, J. Y.,, Cowan, S. W. & Kjeldgaard, M. Improved methods for building protein models in electron density maps and the location of errors in these models. *Acta Crystallogr. A* **47,** 110–119 (1991).
25. Brunger, A. T. *et al.* Crystallography & NMR system: A new software suite for macromolecular structure determination. *Acta Crystallogr. D* **54,** 905–921 (1998).
26. Jogl, G., Tao, X., Xu, Y. & Tong, L. COMO: a program for combined molecular replacement. *Acta Crystallogr. D* **57,** 1127–1134 (2001).
27. Wu, L., Bauer, C. S., Zhen, X. G., Xie, C. & Yang, J. Dual regulation of voltage-gated calcium channels by PtdIns(4,5)P2. *Nature* **419,** 947–952 (2002).
28. Carson, M. Ribbon models of macromolecules. *J. Mol. Graph.* **5,** 103–106 (1987).
29. Nicholls, A., Sharp, K. & Honig, B. H. Protein folding and association: insights from the interfacial and thermodynamic properties of hydrocarbons. *Proteins Struct. Funct. Genet.* **11,** 281–296 (1991).
30. Kraulis, P. MOLSCRIPT: a program to produce both detailed and schematic plots of protein structures. *J. Appl. Crystallogr.* **24,** 946–950 (1991).

Supplementary Information accompanies the paper on **www.nature.com/nature**.

Acknowledgements We thank Y. Mori for $Ca_V2.1$ complementary DNA; E. Perez-Reyes for all β-subunit cDNAs; T. Tanabe for $\alpha_2\delta$ cDNA; and the staff at X4A of NSLS, Brookhaven National Laboratory, for synchrotron support. This work was supported by grants to L.T. and J.Y. from the National Institutes of Health. J.Y. is a recipient of the McKnight Scholar Award, the Scholar Research Programme of the EJLB Foundation and the Established Investigator Award of the American Heart Association.

Competing interests statement The authors declare that they have no competing financial interests.

Correspondence and requests for materials should be addressed to J.Y. (jy160@columbia.edu).
Coordinates have been deposited in the Protein Data Bank under accession codes 1VYU, 1VYT and 1VYV.

corrigendum

Photonic structures in biology

Pete Vukusic & J. Roy Sambles

Nature **424,** 852–855 (2003).

In this Insight Review Article, a reference to earlier work was inadvertently deleted on proof. The omitted citation is Parker, A. R. *Proc. R. Soc. B* **265**, 967–972 (1998). □